Electronic Supplementary Material (ESI) for Journal of Materials Chemistry A.

Supporting Information

Bifunctional VS_2-Ti_3C_2 Heterostructure Electrocatalyst for Boosting Polysulfide Redox in High Performance Lithium-Sulfur Batteries

Yueyue Wang,[a] Yuting Xiong,[a] Qingyi Huang,[a] Zixuan Bi,[a] Zexian Zhang,[b] Zhenzhen Guo,[a] Xianbao Wang[a] and Tao Mei*[a]

[a] *Hubei Collaborative Innovation Center for Advanced Organic Chemical Materials, Overseas, Expertise Introduction Center for Discipline Innovation (D18025), Key Laboratory for the Green Preparation and Application of Functional Materials, Hubei Key Laboratory of Polymer Materials, School of Materials Science and Engineering, Hubei University, Wuhan 430062, PR China *Email: meitao@hubu.edu.cn*

[b] *School of Materials Science and Engineering, Sun Yat-sen University, Guangzhou 510275, China*

Contents

S1 Experimental section

S1.1 Chemicals

Polyvinylpyrrolidone (PVP), ammonium metavanadate (NH_4VO_3, 99.9%), 1,2-dimethoxymethane (DME, 99%), 1,3-dioxolane (DOL, 99.5%), lithium sulfide (Li_2S, 99.9%), acetylene black, polyvinylidene difluoride (PVDF) were purchased from Macklin Biochemical Co., Ltd (Shanghai, China). Ethanol, ammonium hydroxide and HF were obtained from Sinopharm Chemical Reagent Co. Ltd (China). Ti_3AlC_2 was supplied by Shandong Xiyan New Material Technology Co. Ltd. Thioacetamide (C_2H_5NS, 99.0%), N-methyl pyrrolidone (NMP), Tetraethylene glycol dimethyl ether were purchased from Aladdin Industrial Corporation (Shanghai, China). All the above drugs and reagents were supplied by the market without further purification. The deionized water (DI) was purified from ultrapure water machine (Heal Force, China) when the resistance reaches 18.25 $M\Omega \cdot cm^{-1}$.

S1.2 Material synthesis

Preparation of Ti_3C_2 MXene

Ti_3C_2 MXene was obtained through the following process. Specifically, 2 g Ti_3AlC_2 was carefully and slowly immersed in 20 mL 40% HF solution and the reaction was conducted by continuously stirring for 24 h at 25 ℃. Subsequently, the product was centrifuged repeatedly with deionized water until the pH of the supernatant was close to 7. Finally, the sample was freeze-dried for next use.

Synthesis of VS_2-Ti_3C_2 and VS_2

VS_2-Ti_3C_2 was synthesized by one-step hydrothermal method. Briefly, 1.0 g of PVP was dissolved in 30 mL deionized water containing 2.0 mL of ammonium hydroxide solution. Then, 0.002 mol NH_4VO_3 and 0.02 mol C_2H_5NS were added into the above solution and being stirred until dissolved. Next step, 0.1 g mL^{-1} Ti_3C_2 aqueous solution was poured in the above solution, being stirred for 30 minutes and the mixture was put into 50 mL hydrothermal reactor. The reaction was conducted at 180 °C for 20 h. After natural cooling, the precipitate was centrifuged with deionized water and ethanol for several times, and finally, The VS_2-Ti_3C_2 was obtained after being vacuum-dried at 60 °C. The synthesis steps of VS_2 are consistent with the above-mentioned method, without Ti_3C_2 dispersion solution.

Preparation of VS_2-Ti_3C_2/S, VS_2/S and Ti_3C_2/S composites

The main host-sulfur composites were obtained by a facile melt diffusion process. In brief, after uniformly mixing the matrix materials (VS_2-Ti_3C_2, VS_2 and Ti_3C_2) with sulfur powder in a weight ratio (1:4), they were heated at 155 °C for 12 h in Ar atmosphere.

S1.3 Materials characterization

The crystal structure of the material was analyzed by X-ray diffraction (XRD) (D8-advance diffractometer, Bruker, Germany) with Cu Kα radiation. The microstructure of the material was characterized by field emission scanning electron microscope (SEM) (ZEISS, Germany) and transmission electron microscope (TEM) (FEI TECNAI 20, USA). X-ray photoelectron spectroscopy (XPS) (PHOIBOS 150, Germany) was used to analyze the chemical state of elements. Sulfur content was probed using

thermogravimetric analysis technique (TGA) (Diamond TG-DTA, USA) under N_2 atmosphere. UV-vis absorption spectrum was obtained on a UV-3600 Plus spectrometer (UV-3600 Plus, Shimadzu, Japan).

S1.4 Electrochemical measurements

Cell assembly and measurements

To prepare the cathode electrode, the active materials (VS_2-Ti_3C_2/S, VS_2/S and Ti_3C_2/S), PVDF binder and acetylene black were mixed uniformly in NMP at a mass ratio of 7:2:1. The prepared slurry was scraped on carbon-coated aluminum foil, punched into electrode discs with a diameter of 12 mm after vacuum drying at 60 ℃ for 24 h, which were to be assembled into coin-type half cells (CR 2016). The sulfur content of conventional electrode and high loading electrode was about 1.2 mg cm^{-2} and 4 mg cm^{-2}, respectively. The electrolyte/sulfur ratio was typically 13.7 μL mg^{-1}, but dropped to 9 μL mg^{-1} when using cathodes with higher sulfur loadings. Subsequently, lithium sulfur batteries were assembled in an argon-filled glove box. During assembly, metallic lithium foil and Celgard 2400 membrane were used as the anode and separator respectively. The electrolyte was 1.0 M lithium bis(trifluoromethanesulfonyl)imide (LITFSI) with 2 wt% $LiNO_3$ in DOL and DME (v:v=1:1). Galvanostatic charge-discharge tests were operated on LAND CT2001A (Wuhan, China) in a voltage window of 1.7-2.8 V vs. Li^+/Li. Cyclic voltammetry (CV) curves were measured using a CHI760E electrochemical workstation at potential range of 1.7-2.8 V and scan rates of 0.1-0.5 mV s^{-1}. Electrochemical impedance spectroscopy (EIS) curves with scanning frequency from 0.01 Hz to 10^5 Hz were measured.

Preparation of Li_2S_4 solution and visualized adsorption test

The Li_2S_4 solution was prepared by dissolving Li_2S and sulfur (molar ratio =1:3) in a mixed solution of 1,3-dioxolane (DOL) and 1,2-dimethoxyethane (DME) (v/v =1:1) with continuous stirring at 60 °C for 24 h in a glove box filled with Ar gas. The solution finally presents a homogeneous dark yellowish brown. To evaluate the adsorption performance for polysulfides (LiPSs), 10 mg of active materials (VS_2-Ti_3C_2, VS_2 and Ti_3C_2) were added to 4 mL 10 mM Li_2S_4 solution with 30 s shaking and standing for a period of time. the supernatant was characterized by UV-vis and the precipitate was detected by XPS. The above adsorption experiments were carried out in a glove box filled with Ar gas.

Li_2S nucleation and decomposition measurement

The nucleation and dissolution experiments of Li_2S were carried out to study the liquid-solid reaction kinetics. Carbon fiber papers were loaded with about 2.0 mg cm^{-2} carrier material (VS_2-Ti_3C_2, VS_2 and Ti_3C_2) as working electrode and lithium foil as counter electrode. The catholyte contained 25 μL of 1.0 M LiTFSI and 0.2 M Li_2S_8 electrolyte, the latter was synthesized by dissolving Li_2S and sulfur with a molar ratio of 1:7 in tetraethylene glycol dimethyl ether at 60 °C and stirring for 24 h. The anolyte was similar to the catholyte, but did not contain Li_2S_8. During nucleation measurements, fresh cells were galvanostatically discharged to 2.07 V at 0.112 mA. Subsequently, the cell was kept at 2.06 V and potentiostatically discharged until the current dropped to 10^{-5} A for Li_2S nucleation and growth. To investigate the decomposition of Li_2S, the assembled fresh battery was first discharged to 1.7 V with the aim of completely

converting sulfur to Li_2S. Then, the battery was charged to 2.5 V under galvanostatic conditions, and held at 2.5 V until the current dropped to 10^{-5} A.

Theoretical calculations

In the Density Functional Theory calculations (DFT), Vienna Ab initio Simulation Package (VASP) with the projector augmented wave (PAW) method was employed.[1,2] The exchange-functional was treated using the Perdew-Burke-Ernzerhof (PBE) functional, in combination with the DFT-D3 correction.[3,4] Further, the cut-off energy of the plane-wave basis was set at 450 eV. For adsorption of Li_2S and Li_2S_4 on VS_2-Ti_3C_2 3×3×1 supercell surface, the Brillouin zone integration was performed with 2×2×1 Gamma k-point sampling.[5] The self-consistent calculations applied a convergence energy threshold of 10^{-5} eV. The equilibrium geometries and lattice constants were optimized with maximum stress on each atom within 0.01 eV/Å. The isosurface level of charge density difference was 0.01 e $Å^{-3}$. The adsorption energies (E_{ad}) were calculated by the following formula:

$$E_{ad} = E_{total} - (E_{LiPSs} + E_{sub})$$

where E_{total} was the total energy of the configuration with LiPSs, E_{LiPSs} and E_{sub} were the energies of isolated LiPSs species and VS_2-Ti_3C_2, respectively.

S2 Figures and tables

S2.1 Figures:

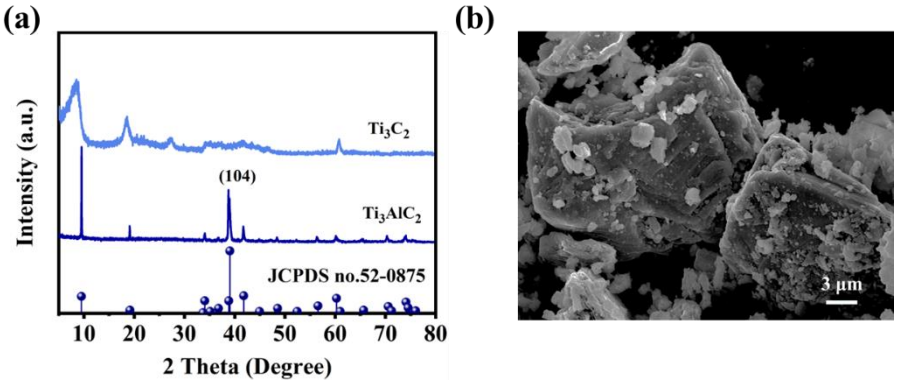

Figure S1. (a) XRD date of Ti_3AlC_2. (b) SEM image of Ti_3AlC_2.

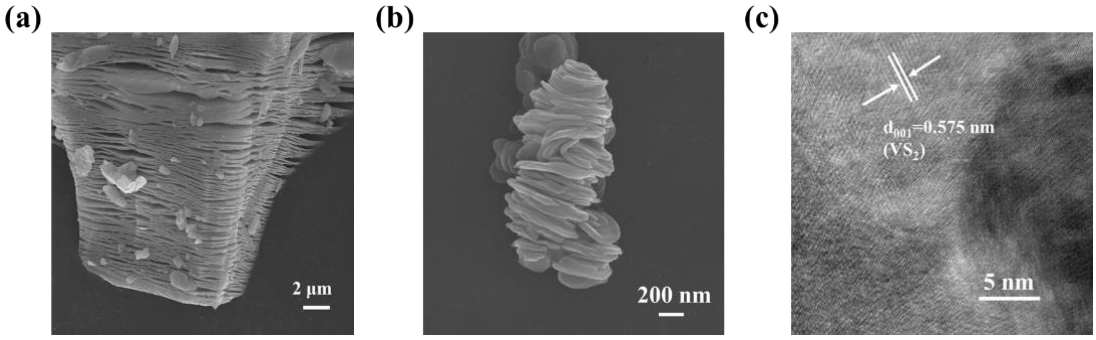

Figure S2. SEM images of (a) Ti_3C_2 and (b) VS_2. (c) HR-TEM image of VS_2.

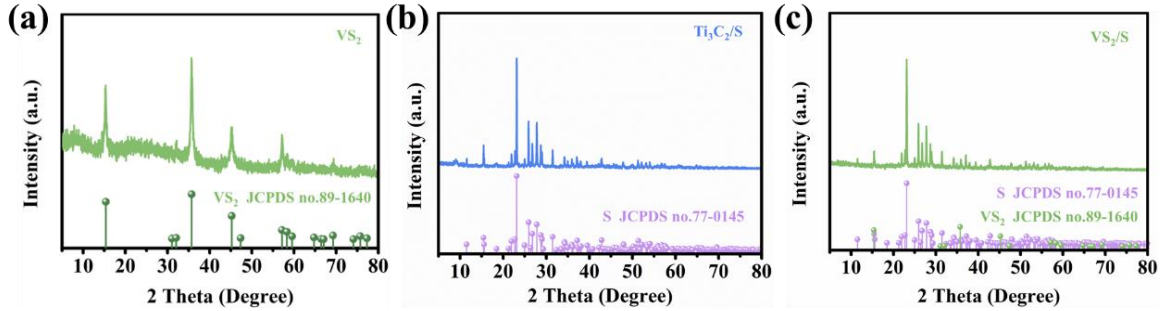

Figure S3. XRD patterns: (a) VS_2, (b) Ti_3C_2/S, (c)VS_2/S.

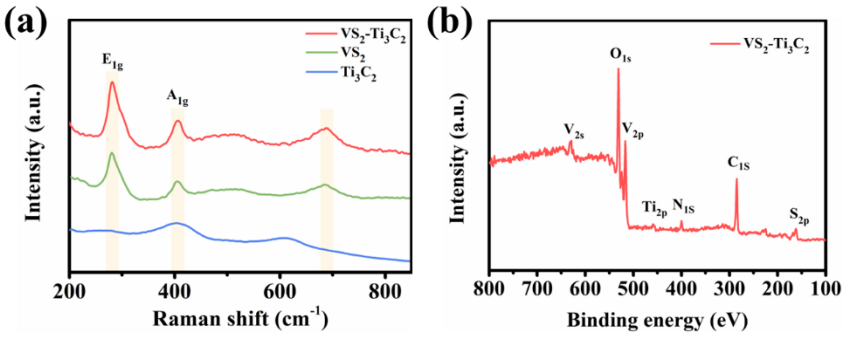

Figure S4. (a) Raman images of VS_2-Ti_3C_2, VS_2 and Ti_3C_2. (b) XPS spectrum of VS_2-Ti_3C_2.

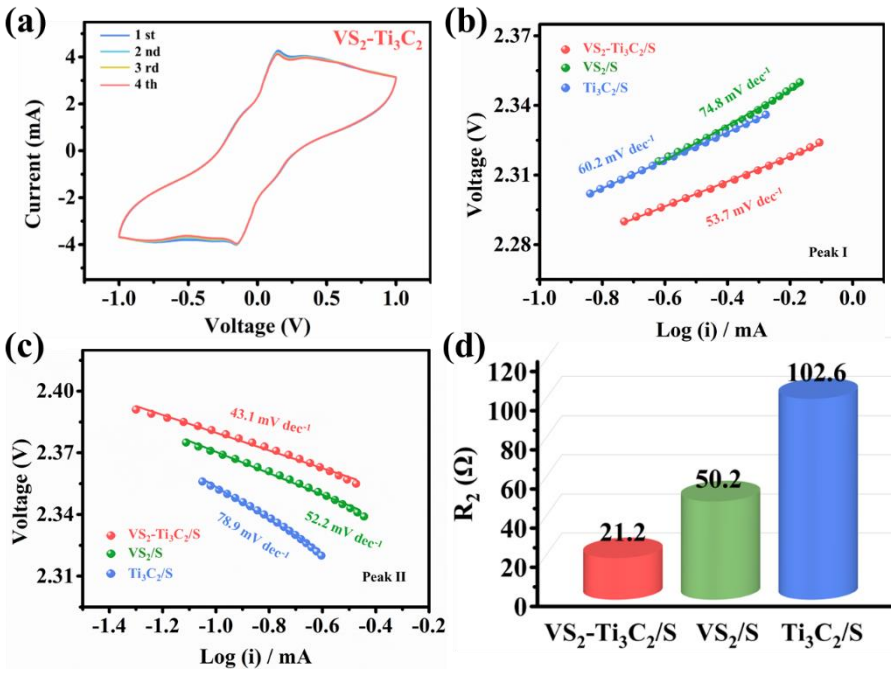

Figure S5. Electrochemical measurement results, (a) The first four CV curves of symmetric cell with VS_2-Ti_3C_2. (b, c) Tafel plots calculated from the peak I and II of CV curves based on VS_2-Ti_3C_2/S cathode materials. (d) Charge transfer resistance (R_2) fitted data of the Nyquist plot of VS_2/S, Ti_3C_2/S and VS_2-Ti_3C_2/S batteries.

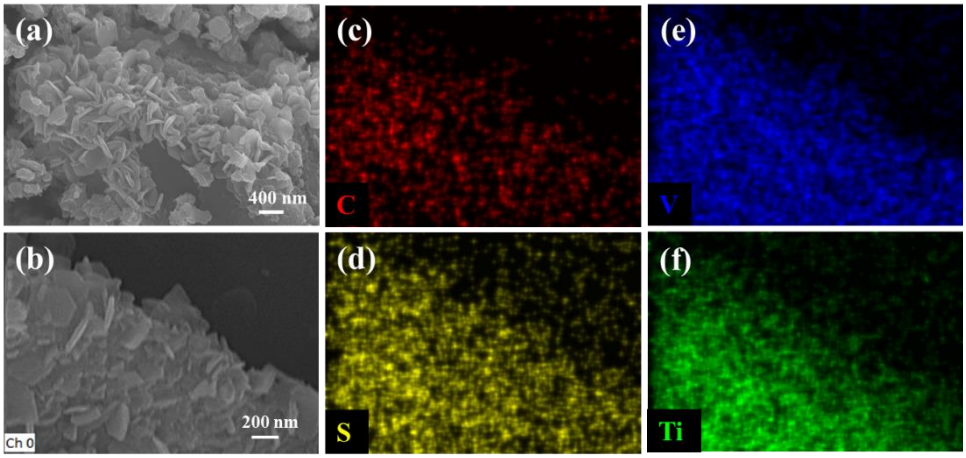

Figure S6. (a-f) SEM images of VS_2-Ti_3C_2 cathode and corresponding EDS elemental mapping for C, S, V, and Ti elements after 500 cycles at 1 C.

S2.2 Tables:

Table S1. Titanium, Vanadium, Carbon, Sulfur, Oxygen atomic percent of VS_2-Ti_3C_2 samples.

Sample	Ti (%)	V (%)	C (%)	S (%)	O (%)
VS_2-Ti_3C_2	30.74	17.01	22.58	25.91	3.76

Table S2. Summary of D_{Li^+} at peaks I, II, III for VS_2-Ti_3C_2/S, VS_2/S and Ti_3C_2/S based LSBs.

CV peak	VS_2-Ti_3C_2/S	VS_2/S	Ti_3C_2/S
Peak I	3.082×10^{-7} cm^2 s^{-1}	2.405×10^{-7} cm^2 s^{-1}	2.036×10^{-7} cm^2 s^{-1}
Peak II	1.201×10^{-7} cm^2 s^{-1}	1.468×10^{-7} cm^2 s^{-1}	7.931×10^{-8} cm^2 s^{-1}
Peak III	1.394×10^{-7} cm^2 s^{-1}	1.401×10^{-7} cm^2 s^{-1}	6.525×10^{-8} cm^2 s^{-1}

Table S3. Summary of recent reports on sulfur host cathodes for LSBs compared to VS_2-Ti_3C_2.

Host material	Specific capacity ($mAh\ g^{-1}$)	(cycles, current rate)	Area sulfur loading ($mg\ cm^{-2}$)	Decay rate (per cycle, %)	Ref
TSC/NbC	937.9	500,0.1C	2	0.037	6
NbS_2@S@IG	856	350,0.5C	1.05	0.07	7
$MoSe_2$@MoO_2	848	500,0.5C	2.3	0.046	8
Co_9S_8@MoS_2	794	400,1C	3	0.091	9
$TiO_2$30-CNFs	723	500,1C	1.5~2	0.041	10
$NiCo_2S_4$@NSCC	710	500,1C	2.0	0.046	11
MCS@Nb_2O_5	650	500,2C	~1.5	0.091	12
$Ti_3C_2T_x$-CNTs	621	500,1C	1.6	0.062	13
Ti_3C_2/C	530	500,1C	1	0.05	14
MNSs@d-Ti_3C_2	501	500,1C	1.2	0.06	15
H-LDH/Co_9S_8	450	500,1C	1.5~2	0.073	16
N-CN@Co_3Se_4	531	800,0.2C	~3.1	0.067	17
$ZnCo_2O_4$@Ti_3C_2	306	400,0.5C	1.0~1.5	0.183	18
S@NG/WSe_2	750.4	500,1C	1	0.037	19
Co-PC@S	798	500,1C	2	0.059	20
S/ZnSe-$CoSe_2$@NC	619.4	400,1C	1.23	0.077	21
$CoNiO_2$/Co_4N-G-S	389	600,4C	1	0.07	22
w-MXene/rGo	837	200,1C	3.43	0.071	23
$MoSe_2$@C/rGO/S	585	300,1C	1.2~1.5	0.1	24
STMn0.3	634	500,1C	1	0.0656	25
GL800/S	631.4	350,0.5C	1	0.079	26
VS_2-Ti_3C_2	**919**	**500,1C**	1.2	**0.024**	**This work**

References

1. J. Hafner, *J. Comput. Chem.*, 2008, **29**, 2044-2078.
2. P. E. Blöchl, *Phys. Rev. B*, 1994, **50**, 17953.
3. J. P. Perdew, K. Burke and M. Ernzerhof, *Phys. Rev. Lett.*, 1996, **77**, 3865.
4. S. Grimme, *J. Comput. Chem.*, 2006, **27**, 1787.
5. H. J. Monkhorst and J. D. Pack, *Phys. Rev. B*, 1976, **13**, 5188.

6. R. Hou, S. Zhang, P. Zhang, Y. Zhang, X. Zhang, N. Li, Z. Shi and G. Shao, *J. Mater. Chem. A*, 2020, **8**, 25255-25267.
7. S. Shen, X. Xia, Y. Zhong, S. Deng, D. Xie, B. Liu, Y. Zhang, G. Pan, X. Wang and J. Tu, *Adv. Mater.*, 2019, **31**, 1900009.
8. Z. Xiao, Z. Yang, L. Zhang, H. Pan and R. Wang, *ACS Nano*, 2017, **11**, 8488-8498.
9. Q. Hao, G. Cui, Y. Zhang, J. Li and Z. Zhang, *Chem. Eng. J.*, 2020, **381**, 122672.
10. B. Li, Q. Su, L. Yu, J. Zhang, G. Du, D. Wang, D. Han, M. Zhang, S. Ding and B. Xu, *ACS Nano*, 2020, **14**, 17285-17294.
11. T. Sun, C. Huang, H. Shu, L. Luo, Q. Liang, M. Chen, J. Su and X. Wang, *ACS Appl. Mater. Interfaces*, 2020, **12**, 57975-57986.
12. Y. Tao, Y. Wei, Y. Liu, J. Wang, W. Qiao, L. Ling and D. Long, *Energy Environ. Sci.*, 2016, **9**, 3230-3239.
13. M. Xu, L. Liang, J. Qi, T. Wu, D. Zhou and Z. Xiao, *Small*, 2021, **17**, 2007446.
14. H.Y. Zhou, Z.Y. Sui, K. Amin, L.W. Lin, H.Y. Wang and B. H. Han, *ACS Appl. Mater. Interfaces*, 2020, **12**, 13904-13913.
15. H. Zhang, Q. Qi, P. Zhang, W. Zheng, J. Chen, A. Zhou, W. Tian, W. Zhang and Z. Sun, *ACS Appl. Mater. Interfaces*, 2018, **2**, 705-714.
16. S. Chen, J. Luo, N. Li, X. Han, J. Wang, Q. Deng, Z. Zeng and S. Deng, *Energy Storage Mater.*, 2020, **30**, 187-195.
17. D. Cai, B. Liu, D. Zhu, D. Chen, M. Lu, J. Cao, Y. Wang, W. Huang, Y. Shao, H. Tu and W. Han, *Adv. Energy. Mater.*, 2020, **10**, 1904273.
18. A. Wei, L. Wang and Z. Li, *J. Alloys Compd.*, 2022, **899**, 163369.
19. C. Q. Zhang, B. Fei, D. W. Yang, H. B. Zhan, J. A. Wang, J. F. Diao, J. S. Li, G. Henkelman, D. P. Cai, J. J. Biendicho, J. R. Morante and A. Cabot, *Adv. Funct. Mater.*, 2022, **32**, 2201322.
20. 20 Y. F. Xue, D. Luo, N. Yang, G. Ma, Z. Zhang, J. F. Hou, J. T. Wang, C. Y. Ma, X. Wang, M. L. Jin, Z. W. Chen and L. L. Shui, *Chem. Eng. J.*, 2022, **440**, 135990.

21. J. Xu, L. L. Xu, Z. L. Zhang, B. Sun, Y. Jin, Q. Z. Jin, H. Liu and G. X. Wang, *Energy Storage Mater.*, 2022, **47**, 223-234.
22. J. Pu, W. B. Gong, Z. X. Shen, L. T. Wang, Y. G. Yao and G. Hong, *Adv. Sci.*, 2022, **9**, 2104375
23. C. Y. Zhang, W. Chu, X. F. Hong, Q. He, R. H. Lu, X. B. Liao and Y. Zhao, *Chem. Eng. J.*, 2022, **439**, 135679.
24. C. C. Li, W. N. Ge, S. Y. Qi, L. Zhu, R. Z. Huang, M. W. Zhao, Y. T. Qian and L. Q. Xu, *Adv. Energy. Mater.*, 2022, **12**, 2103915.
25. W. S. Hou, P. L. Feng, X. Guo, Z. H. Wang, Z. Bai, Y. Bai, G. X. Wang, and K. N. Sun, *Adv. Mater.*, 2022, **34**, 2202222.
26. J. Q. Cui, J. Liu, X. Chen, J. S. Meng, S. Y. Wei, T. Wu, Y. Wang, Y. M. Xie, C. Z. Lu and X. C. Zhang, *Carbon*, 2022, **196**, 70-77.